Ann. For. Res. 66(1): 2639-2661, 2023
ISSN: 18448135, 20652445

ANNALS OF FOREST RESEARCH
www.e-afr.org

ADSORPTION OF CIPROFLOXACIN ANTIBIOTIC BY LOW COST MATERIAL / ISOTHERM, KINETIC AND THERMODYNAMIC STUDY

Ahmed Abdulmalk Fayyad*, Khalid Khazal Hummadi
Department Environmental Engineering, college of Engineering , University of Baghdad , Iraq.
*Ahmed.Fayyad2011M@coeng.uobaghdad.edu.iq

Abstract

In this work, locally and natural porcelanite rock (PC) investigated as an adsorbent media for Ciprofloxacin (CIP) removal from aqueous solutions in batch and continuous fluidized bed column. Using different techniques including FTIR, and XRD, SEM, and BET porcelain rock characterizations were performed. pH, contact time, initial antibiotic concentration, dosage, and particles size has been investigated in the batch mode system. FTIR analysis shows that the main function group of PC responsible for the adsorption mechanism was silanol-OH and Si-OH-Si. XRD analysis revealed that PC compound is mostly quartz. Surface morphology shows a wide variety of intragranular pores relatively to the high porosity of PC also, indicating high surface areas. PC have suitable surface area of 6.8402 m^2/g, volume of Pore of 0.015319 (cm^3/g), and Average pore diameter of 9.8129 (nm)**.** In batch system mode the optimal parameters were; pH = 5. PC dose = 0.02 g/ml, particles size = 425 µm, and 120 min detention time. The removal efficiencies of CIP increased dramatically as the starting concentration increased and the best removal percent was 93.36% at 90 mg/l. Thermodynamic study state that there is no significant effect of temperature on the CIP adsorption. The negative value of ΔG represent the viability and spontaneity of adsorption process. Positive value of ΔH and ΔS indicated that the endothermic adsorption nature, and perfect affinity of adsorbate to adsorbent. Isotherm study state that the maximum adsorption capacity of CIP onto PC is 20.20977 mg/g. RL value (0<RL<1) state the adsorption is favorable process. Freundlich intensity (n>1) suggested that the adsorption is preferential. Langmuir Model is the more fitted model that has the largest value of R^2 of (0.98539). Second-order is the more fitted kinetic model to describe the adsorption behaver.

Keywords: Adsorption · porcelanite rock · Ciprofloxacin · Isotherm· Kinetic.

1. Introduction

Although the many benefits of pharmaceuticals and higher consumption in human and veterinary medicine and so forth, the release of the effluents containing these compounds from different sources has caused the accumulation of these materials and their residuals, especially antibiotics and their metabolites; this a major challenge to the public health and environmental [1]. The studies point out the continuous introduction to sewage waters of these compounds along with their metabolites and the inefficiency of many conventional wastewater treatment plants (WWTPs) in their removal [2, 3]. This antibiotic is very harmful to the environment because of its high solubility at different pHs and high stability [4]. This matter has been detected at the low ng/l level in rivers and lakes to 50 grams in the effluents of pharmaceutical factories [3, 5].Conventional

methods have their own limitations in treating pharmaceutical wastewaters containing a wide range of solvents and toxic materials [1]. One of the largest groups of antibiotics which have strong chemical stability and consequently are not fully metabolized in the body is Fluoroquinolones (FQs). FQs are excreted in urine and animal excrement and eventually discharged into wastewater treatment plants (WWTPs). FQs revealed toxic effects on microbial activity thus they are often poorly biodegradable in biological treatment systems [6].

Ciprofloxacin (CIP) as the second generation of fluoroquinolones (FQs) is a synthetic antibiotic and has been widely used for the treatment of bacterial infectious disease in humans and animals. The lake of appropriate treatment systems in conventional wastewater treatment plant of drug manufacturers and hospitals and on the other hand unsuitable disposal of unused or expired CIP and incomplete metabolization of it in humans severely result in increasing the CIP contamination of surface water in the last decade [7]. Literature surveys revealed that many research groups focused on developing an efficient and economical procedure for CIP contamination removal from drinking water supply and wastewaters before releasing them into the environment. Since CIP is resistant to microbial metabolism, it cannot be efficiently degraded by means of biological treatment processes [8].They can cause microbial resistance among pathogen species or the death of microorganisms that are successful in wastewater treatment when antibiotics enter wastewater and drinking water [9]. The elimination of antibiotics from wastewater or drinking water is important. It is necessary and right to extract antibiotics from infected water before releasing them into the environment, but it's fairly costly.

There are many techniques applied to remove antibiotics from aqueous solution, such as: the ion exchange [10], advanced oxidation process [11] , adsorption [12] , photodegradation [13] , biodegradation [14] and electrocoagulation [15]. Among these techniques presented, Adsorption is an effective technique used widely to treat low antibiotic concentration. The adsorption process is one of the most efficient methods of removing pollutants from wastewater. Also, the adsorption process provides an attractive alternative treatment, especially if the adsorbent is inexpensive and readily available [16, 17]. Activated carbon is the most widely used adsorbent for the removal of pollutants from effluents because it has a high capacity for organic matter, but its use is limited due to its high cost. This cost problem has led to a search for the use of alternate cheap and efficient materials [18]. However, the adsorption capacity of the adsorbents is not very large; to improve adsorption performance new adsorbents are still under development. For the adsorption process to be integrated in terms of removal efficiency and economic feasibility, the adsorbent should be chosen with great care [19]. Several studies have evaluated natural materials as an adsorbent medium, such as rocks or clays, so this research aims to experiment with a natural porcelain stone as a low-cost adsorbent. The method of adsorption is typically performed in batch and continuous systems. The batch process offers useful knowledge of the best Operational conditions that will be functional in the continuous system.

2. Materials and Methods

2.1 Adsorbents

The material that were utilized as adsorbent is a Porcelanite rock (PC) which is a natural sorbent have been brought from the Iraqi Ministry of Industry, Geological Survey Department. PC was broken manually and washed by distilled water and let it to dry completely then it sieved to a different particle size range (425, 600,1180,1700,2360, and 4750μm) as shown in fig 1.

Table 1 : Chemical Characteristics of Sorbent (State Company of Geological Survey and Mining, Mining Centre).

Sample no.	CaO%	$Si\mathbf{O_2}$%	$A\boldsymbol{l_2O_3}$%	$F\boldsymbol{e_2O_3}$%	MgO%
Porcelanite	11.55	62.02	2.71	0.87	2.7

a **b**

Figure 1 : Porcelanite rock Before (a) and After Cracking (b).

2.1 Adsorbate

Ciprofloxacin(C17H18FN3O3, solubility in water 36 mg mL−1 at 25°C, molecular weight 331.35 g mol−1, wavelength 272 nm, purity ≥98%). Ciprofloxacin (CIP) were used in this study as adsorbate material which is among the most common antibiotics using in many different purpose. CIP was collected locally from pharmacies since it is the final discarded to environment. Stock solution of ciprofloxacin was prepared by dissolving an appropriate quantity of powdered antibiotic in 1 L of distilled water (Due to the instability in the laboratory conditions) the stock and diluted solutions were prepared at the time of the experimental work. The pH value of solutions was controlled during the experiments by drop wise addition of 0.1 M NaOH or HCl.

2.3 Instruments and Measuring Devices

Spectrophotometer (advanced microprocessor UV-VIS spectrophotometer single beam LI-295): used to measure the concentrations of soluble (ciprofloxacin solution).the characteristic wavelength used 270 nm. PH Meter (WTW, Bench model, German): for measuring the pH of the solution samples. Shaker Incubator ((Edmund Buhler SM25, German): has shaking speed changed from 50 to 300 rpm. FTIR Fourier Transform Infrared Spectroscopy (IRAFFINITY-1,SHIMADZU). SEM Scanning Electron Microscopy use (NOVASEM, FEL450L) analysis under 10 KV voltage and a 6-mA flux. XRD (X-Ray Diffractometer) 2700AB HAOYUAN co., China. Electrical Balance (type: Sartorius) Digital Indicator with capacity (210 g) was used for weighting the materials.

3. Batch Experiments

Adsorption Experiments

Case a known weight of ciprofloxacin (CIP) were added to conical flask of 250 ml volume. The PH of solution was adjusted to preferred value by adding 0.1M of (NaOH or HCl). A known weight of sorbent was added to flask, after that the flask were put in shaker and agitated continually in 300 rpm at 25°C temperature and for desired time, after test, the samples were withdrawn and filtered by qualitative filter paper(rate of percolation: medium, model 102). The spectrophotometer to measure the effluent concentration. Removal efficiency was estimated by the following equation [7].

$$\text{Removal } \% = [(Co - Ce)/C_o] * 100 \quad (1)$$

Where:

Co: the initial concentration of CIP, ppm. Ce: the effluent concentration of CIP at any time, ppm. The rang of all parameters which used in the batch experiments are listed in table 2 .

Table 2 : Batch experiment parameters and it is range.

batch Experiment Parameters	Ranges
pH	2, 3, 4, 5,6,7,8 and 10
Initial concentration	10, 30, 50, 70 and 90
Particle size(µm)	425,600,1180,1700,2360, and 4750
Dosage(g/ml)	0.001, 0.002, 0.004,0.006,0.008,0.01,0.02 and 0.03
Time(min)	10-200
Shaking speed (rpm)	Constant at 200

4. Results and Discussion

4. 1 Adsorbent Characteristics

4.1.1 FT-IR Analysis of Adsorbent

FTIR analysis of PC was performed in order to identify the processes that lead to CIP adsorption. The spectra of untreated and treated PC samples are shown in Figure (2.a). The broad band identified at 3667.47- 2918.00 cm^{-1} can be assigned to the O-H group [20] . The band at 1650.45 cm^{-1} could be attributed to the deformation of water molecules (H_2O). A less strong band, caused by the bending of H-O-H, has been seen at 1650.45 cm^{-1} [21] . Calcite can be recognized in the present samples of PC due to doubly degenerate asymmetric stretching vibration at a wavenumber of 1392.17 cm^{-1} and C=O stretching at 512.88 cm^{-1} [22] . The FT-IR spectra shows existence of the terminal silanol-OH and to the bright Si-OH-Si this might have influence on the adsorption process. the characteristics peaks show Si-O groups at 558.97 cm^{-1} and CO_3 at 1456.14 cm^{-1} [23] . The band at 1167.10 cm-1 that appear as strong band can be assigned to the symmetric (Si-O-Si) or asymmetric (Si-O-Si) stretching vibrations [24] . The bands at 781.11 cm^{-1} are characteristic of Quartz and those at 468.74 cm^{-1} can be attributed to Si-O-Si bending vibrations [24] . The sharp bands near 455 cm^{-1} define the Si–OH stretches. The Peak displacement increasing after adsorption (figure 2.b) define the change in the structure with CIP imply the related functional groups to be responsible for the adsorption process. The results show that the bands of silanol-

OH and Si-OH-Si groups shifted to upper displacement and therefore it plays the major role in adsorption process. The bands of functional groups shifted to upper wavenumber with a total amount of 1167.8, 780, 552.2, and 468.61 cm^{-1} for PC loaded with TTC.

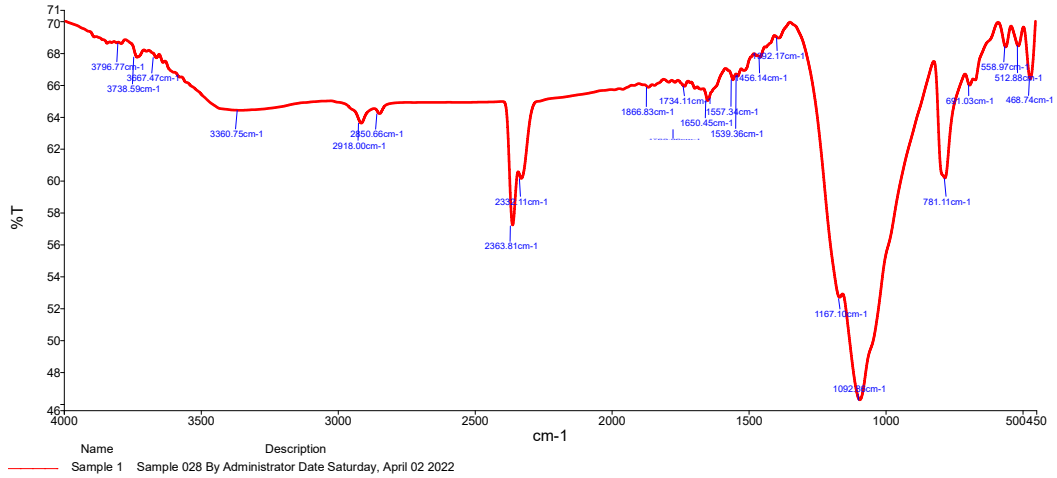

Figure 2 a : FTIR Analysis of Raw PC adsorbent.

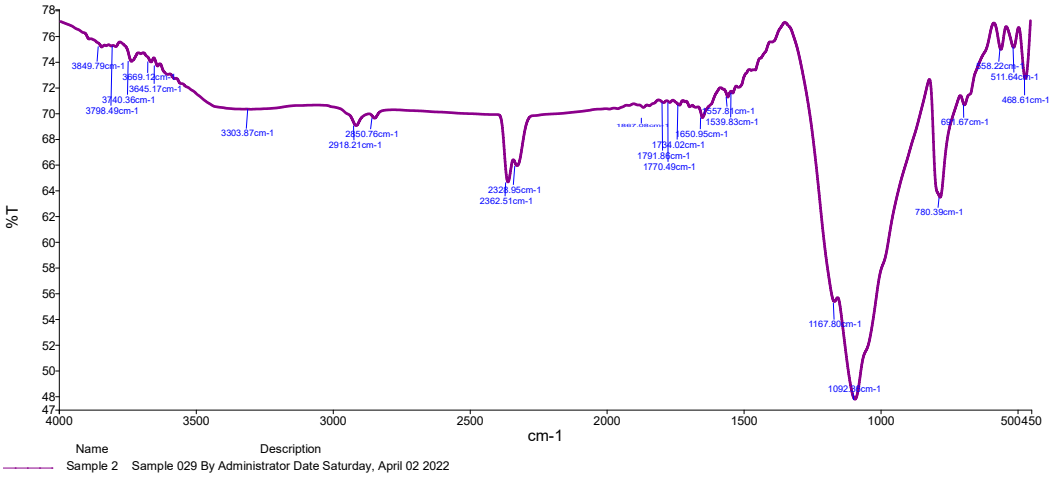

Figure 2 b : FTIR Analysis of PC adsorbent after adsorption.

4.1.2 XRD analysis of adsorbent

X-ray diffraction(XRD) is a technique for analyzing the atomic or molecular structure of materials. It is non-destructive and works most effectively with materials that are wholly, or part, crystalline. The X-ray diffraction test results of PC rocks give data in the form of 2θ diffraction angle and intensity as shown in Fig (3.a). The diffraction pattern shows the existence of 15 diffraction peaks. The main peaks were at the position of (2θ) 20.7, 26.5, 36.5, 39.4, 50, 68, and 75.64. The X-ray diffraction (XRD) pattern confirms the presence of many compounds in the chemical composition of sand. The mainly compound is quartz with a chemical formula SiO_2. As shows in figure (3.b), there's no obvious difference between the result of the raw and adsorbent XRD tests. That means there was no change in the chemical composition of PC, suggested that physical adsorption is the control of the removal process.

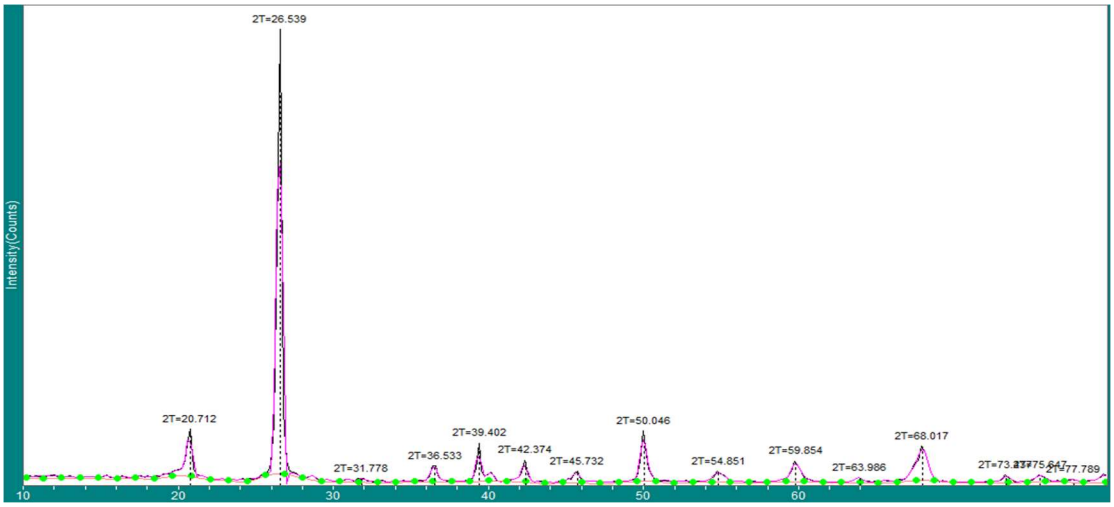

Figure 3.a : XRD Pattern of Raw PC adsorbent

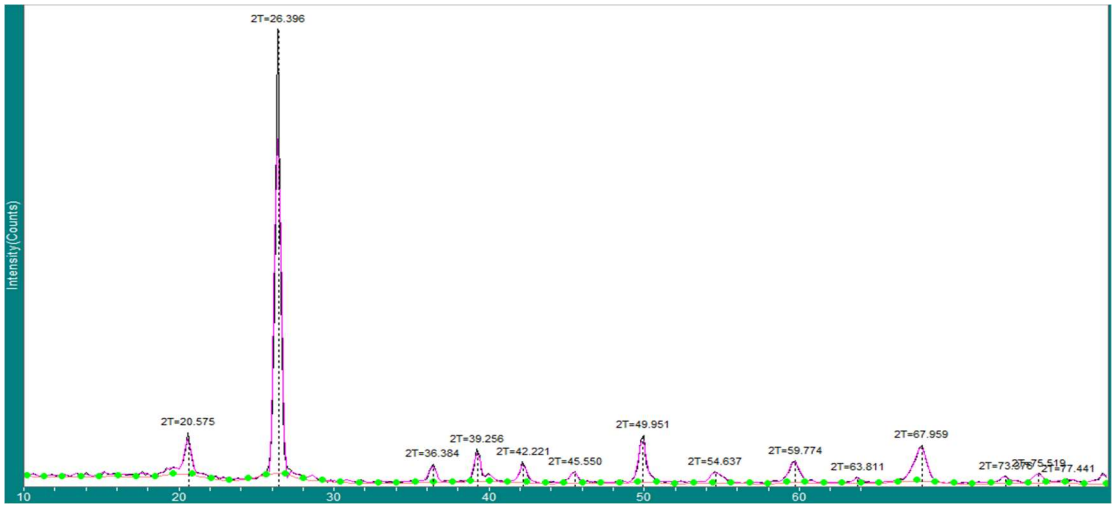

Figure 3.b : XRD Pattern of PC adsorbent after adsorption.

4.1.3 SEM Analysis of Surface Morphology

Scanning electron microscope (SEM) is a type of electron microscope that produces images of a sample by scanning the surface with a focused beam of electrons. To understand more about the surface morphology, microstructures and crystalline phases of PC, SEM analysis were subjected before and after the adsorption process. SEM investigation of PC shows a wide variety of irregular sizes and shapes of grains as showed in figure (4.a). There is also a wide variety of size and shape of intergranular pores. The comparatively high porosity of these PC is attributed to the combination of irregular size and shape of grains and the high amount of intergranular porosity also, indicating high surface areas. Noted that the surface shape after adsorption is more uniform and consistent compared to raw PC this may be due to the contaminants that filled these holes and grooves as showed in figure (4.b).

Surface area of any adsorbent is detected by Brunauer–Emmett–Teller (BET) method. The result show that the PC have suitable surface area of 21.63m²/g. The Berrett-Joyner-Halenda (BJH) technique accustomed to limit the pore size distribution**.** For raw PC, the volume of pore was 0.072 (cm³/g), also the Average pore diameter of 8.96 (nm)**.**

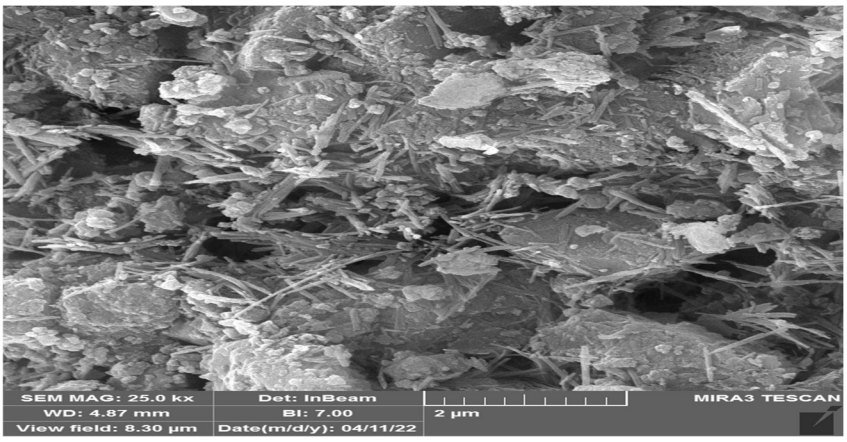

Figure 4.a : Surface Morphology of Raw PC adsorbent

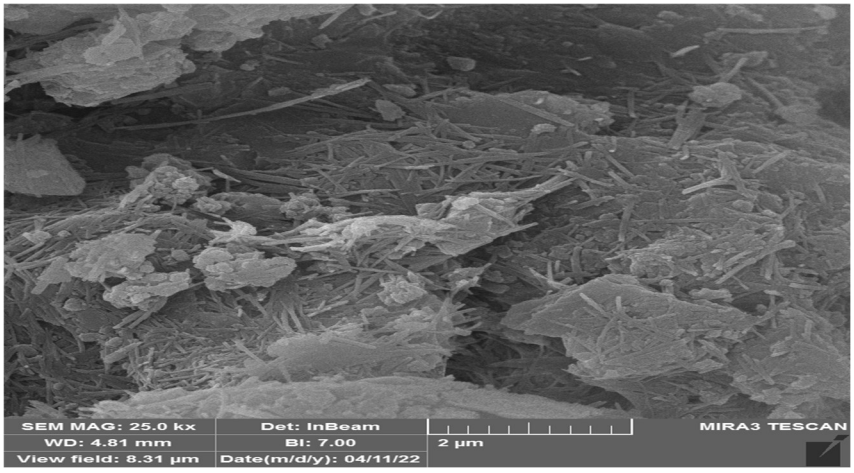

Figure 4.b : Surface Morphology of PC adsorbent after adsorption

4.1.4 EDS Analysis of Adsorbent

Energy-dispersive X-ray spectroscopy (EDS) is an analytical technique used for the elemental analysis or chemical characterization of a sample. It relies on an interaction of some source of X-ray excitation and a sample. Elemental analysis for the PC before and after adsorption were carried out by EDS. The EDS analysis figs (5.a & 5.b) shows the existence of several elements in the adsorbent surface before and after adsorption: Oxygen (32%), Silicon (54.13%), Magnesium (7.56%), Phosphorus (1.94%), and S (11.93%). After adsorption there are various elements were appeared in EDS analysis: Carbon (5.09 %), Oxygen (32.75%), Silicon (53.5%), Magnesium (1.6%), Phosphorus (2.8%), S (11.93%), and Al (1.67%). The Carbon appearance may be due to the organic composition of CIP molecules that loaded on PC surface. In contrast, the high ratio of Si before and after adsorption made the EDS analysis compatible with the FTIR (The

major functional groups present in the samples were Si-O-Si groups) and XRD (The mainly compound is quartz with a chemical formula SiO_2).

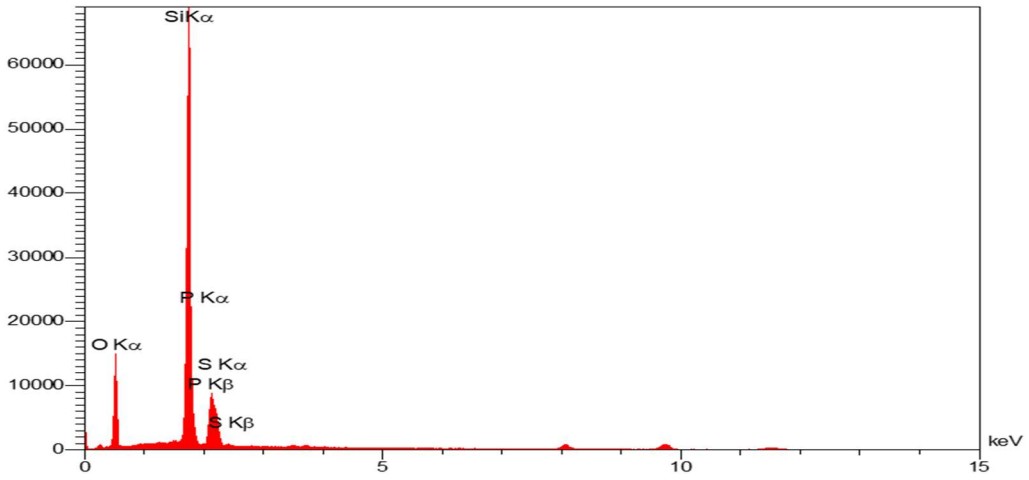

Figure 5.a : EDS analysis of Raw PC adsorbent.

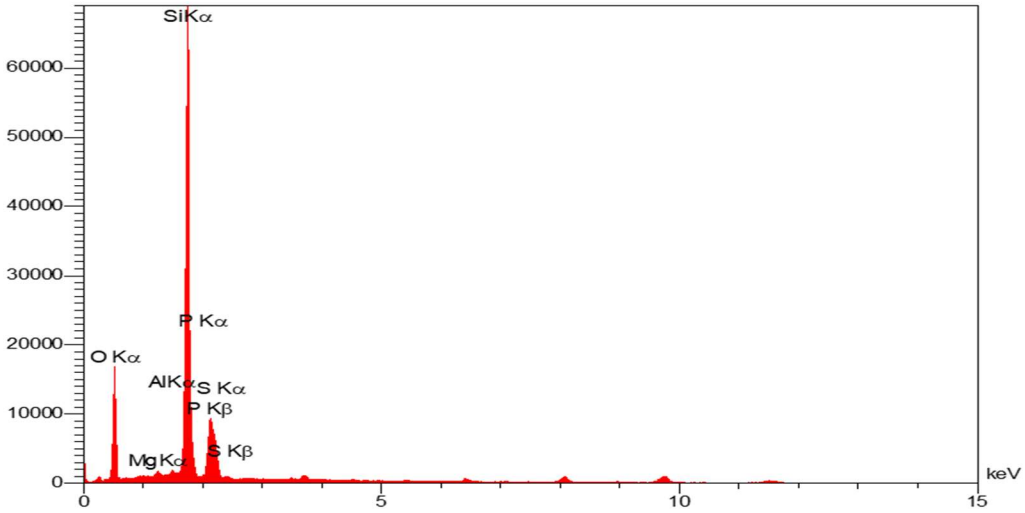

Figure 5.b : EDS analysis of PC adsorbent after adsorption.

4.2 Batch mode experiment

4.2.1 Effect of pH

To achieve the optimal removal efficiencies, solutions at different pH values between 2 and 10 were examined for the impact of pH. By combining the appropriate amount of adsorbent (0.02 g/ml), it was possible to determine how pH affected the adsorption of CIP with 50 mg/l. Generally, the pH values determine the effectively any pollutant removal from aqueous solution in adsorption process [25] .Hydrogen ions concentration in solution is a vital consideration for the adsorption process. Ionization degree of the adsorbent and adsorbate are both influenced by pH, which also replaces a number of the positive ions found in the active sites [26, 27] . Point of zero charge (pzc) represent

the pH value at which the total net charge of absorbent's surface equal to zero. Consequently, at pH values are lower than pHpzc, the adsorbent's surface charge is positive, and vice versa [27] . Due to electrostatic repulsion, the cations adsorption, is favorite when pH > pHpzc, whereas the anions adsorption is favored at pH pHpzc [28] . So as, the detection of pH value at which the adsorbent surface being neutral charge is significant choice (Figure 6.a). According to analysis, the pH_{pzc} of the PC was determined to be 7.2 where the PC behaves as neutral surface. It was observed that CIP adsorption increased from 59.9 % to 91.2% when the pH solution increased from 2 to 5 after that the adsorption percent gradually reduced to 96 % at a solution pH of 10. The adsorption of the negative charge of CIP is favored at pH < pHpzc because high electrostatic attraction exists between the positively charged surface of the adsorbent and pollutant reported a high removal percent. At pH lower than 7.2 the adsorbent surface protonated and the adsorbent surface becomes positively charge, thus the electrical attraction take place between the PC and the negatively charge groups of CIP. The optimum CIP capacity was obtained when the pH is around 5 as displayed in figure (6.b). This observation could be attributed to a strong electrostatic force of attraction between positively charged adsorbed surface and CIP ions in acidic media. Reducing in adsorption onto PC surface at higher than pH 5 resulted from the repulsion between molecules of adsorbate and PC surface that being negatively charged in alkaline media.

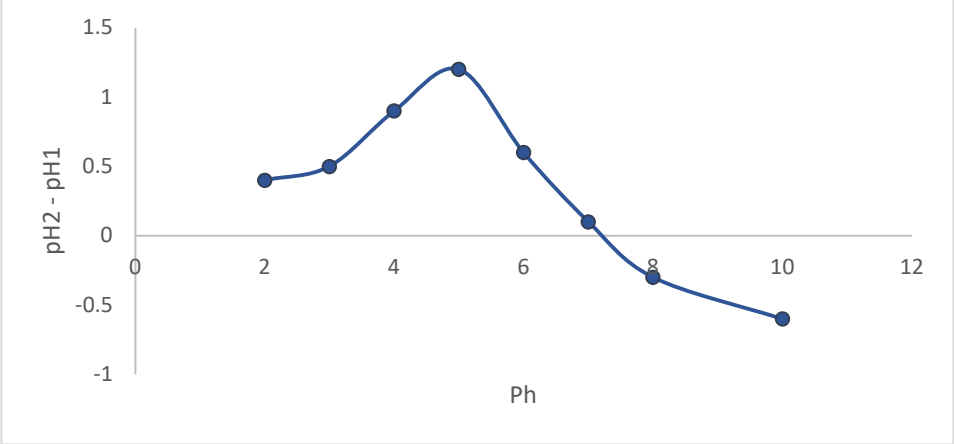

Figure 6.a : zero charge point of Porcelanite Rocks.

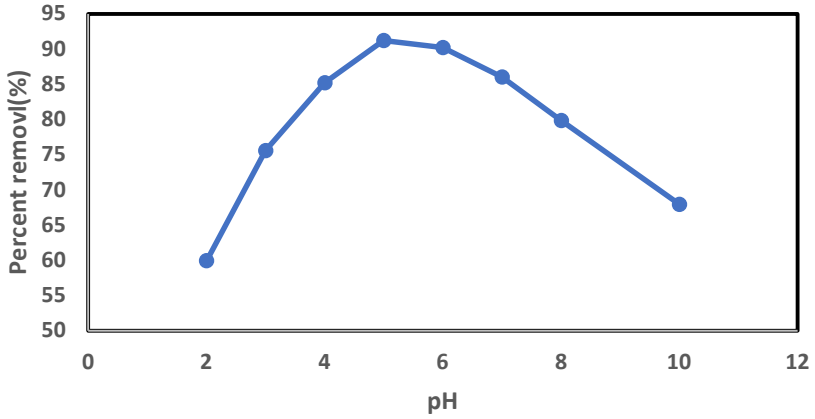

Figure 6.b : Effect of pH on CIP removal efficiency; Co=50 mg/l, particle size= 424 µm, T=25 Co, dosage= 0.02g/ ml, and t= 120 min and rpm 300.

4.2.2 Effect of Dosage

Adsorbent dose is an important parameter because it determines the capacity of the sorbent for a given initial concentration of the adsorbate [28] . Fig (7) shows the relationship between PC adsorbent dose and removal efficiency with contact time. The experiment results revealed that the removal efficiency of CIP increased from 17.04 % to 92.2 % as the PC adsorbent dose increase from 0.001 to 0.05 g/ml due to the availability of more binding sites on the adsorbent surface, after this point the adsorption tend to be steady state process. The non-significant rate of elimination may be due to adsorption sites overlapping or aggregating that Result decreasing in the total adsorbent surface area [29] . Therefore, 0.02 g/ml was selected as the optimum dose because it gives a suitable removal by the consumption of a fit amount of PC.

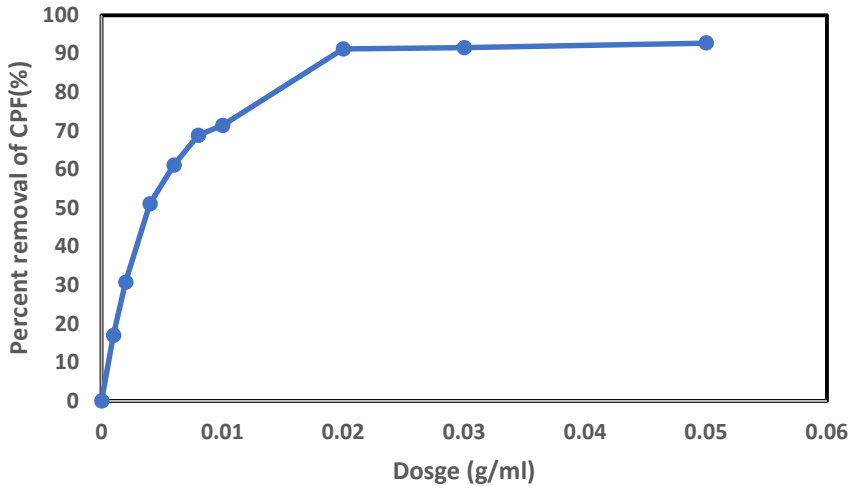

Figure 7 : Effect of dosage on CIP removal efficiency; Co=50 mg/l, particle size= 424 µm, T=25 Co, pH= 5, time= 120 min and rpm 300.

4.2.3 Effect of Particles Size

Surface area of the sorbent is an important parameter for sorption [29] . Fig 8 shows the relationship between the particle size of the sorbent and antibiotic removal efficiency. The results show that the removal efficiency, decreased with the increased in particle size from 425 to 4750 µm from 91.2 % to 50.56 %. This is recognized to the fact that smaller particle sizes give larger surface areas which allow rapid adsorption. Mass transfer diffusion resistance is larger for large particles as a smaller size lets very fast removal kinetics if the adsorption is to be mainly a surface phenomenon [29] .

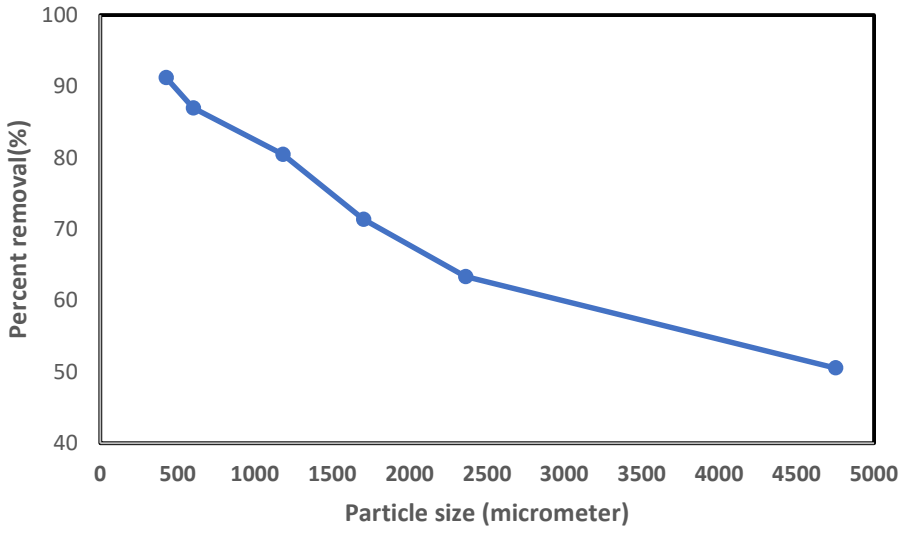

Figure 8 : Effect of particle size on CIP removal efficiency; Co=50 mg/l, pH= 5, T=25 Co, dosage= 0.02g/ml, time= 120 min and rpm 300.

4.2.4 Effect of time and Initial Concentration

The PC's adsorption ability was investigated by varying the contact time from 10 to 200 min. The results show that the adsorption for 10 min was rather fast and reached the state of equilibrium at above 80 min. after this point, the adsorption process tends to be roughly constant for removal percent. The removal percentage has increased from 77.7% to 80. 3% as the time increased from 80 to 200 min for an initial concentration of 10mg/l. While increased from 91.07% to 91. 86% for an initial concentration of 50mg/l and increased from 91.12% to 92.82% for an initial concentration of 90mg/l. Therefore, results indicated that 80 min was the best time for the adsorption of CIP onto the PC.

The effect of the CIP initial concentrations of (10, 30, 50, 70, and 90) mg/l on the removal percent of CIP onto PC was examined. The removal efficiencies of CIP increased dramatically as the initial concentration increased as shown in Fig 9 . After 10 min, the removal percent increased

from 50 to 85.23% as the initial concentration increased from 10 to 90 mg/l. Also after 80 min, removal percent increased from 77.7 to 91.12% when the concentration increased from 10 to 90 mg/l and increased from 80.3 to 92.86% after 200min with increasing the concentration from 10 to 90 mg/l. This was caused by the high concentration gradients that this has emerged at the greater adsorption, increase initial concentration gives a high driving force to transport the CIP molecules from the solution to the adsorbent surface [30 ,31].

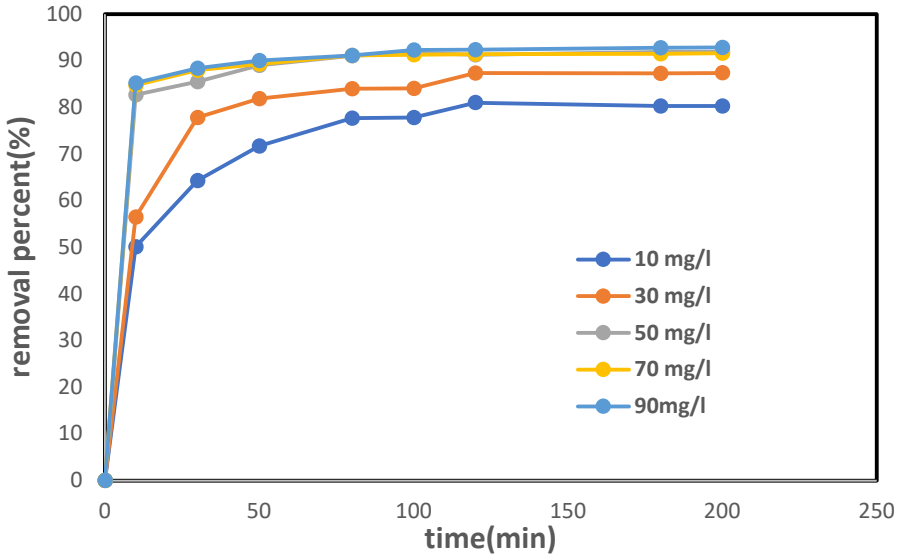

Figure 9 : Effect of Initial Concentration on CIP removal efficiency; Co (10-90) mg/l, particle size (424) µm, Temp. (25) ºC, dosage (0.02) g/ml, pH 5, time(10-200)min. and rpm 300.

4.3 Thermodynamic study

The parameters of thermodynamic change of standard Gibbs free energy (ΔGº), enthalpy (ΔHº) and entropy (ΔSº) were calculated using the following equations [12]:

$$\Delta G^{\circ} = -RT \ln Kc \quad (2)$$

$$\Delta G^{\circ} = \Delta H^{\circ} - T\Delta S^{\circ} \quad (3)$$

$$ln(k_c) = \frac{\Delta S^{\circ}}{R} - \frac{\Delta H^{\circ}}{RT} \quad (4)$$

$$K_c = \frac{q_e}{c_e} \quad (5)$$

Where: ΔHº enthalpy change (kJ/mol), ΔSº entropy change (kJ/mol.K), ΔGº is a free energy change (kJ/mol); (R is 8.314 J/mol K), T the temperature in kilven(k), Kc (L g^{-1}) the equilibrium constants(L g^{-1}) , ΔSº values in the adsorption process which are dogged from the intercept and slope of the plot of ln(Kc) versus 1/T, respectively [19]. The Gibbs free energy shows that the degree of feasibility and spontaneity of the adsorption procedure. Reactions occur spontaneously at a given temperature if ΔG° is a negative quantity. Where the negative values

redirect a more energetically favorable adsorption process. ΔGº decrease with T increasing indicated the endothermic adsorption process and it is chosen with temperature increasing, the opposed situation (ΔGº increase with T increase) clarified that the exothermic adsorption process and so favored besides temperature decreasing [19]. Temperature is a significance parameter on sorption process. The higher temperature contributes to an increase in the rate of diffusion of adsorbed molecules through the outer boundary layer and the internal pores of the adsorbent particles. The temperature effect on the removal efficiency of the antibiotic studied has been investigated at temperature range of (25-45°C). Fig 10 shows the change of removal efficiency of antibiotic with respect to varying temperature values. It was noticed that there is no significant effect of temperature on the removal efficiency. Removal percent increase slightly from 91.074 % to 92.28% as the solution temperature increases from 25 to 45ºC with condition of (Co (50) mg/l, particle size (424) µm, time (80) min and dosage (0.02) g/ml). The findings revealed that CIP adsorption is endothermic. In boating enough energy, the number of molecules is increased to undergo interaction with active site on the surface [32] .

The thermodynamic parameters measured are Gibbs free energy ΔG, enthalpy ΔH, entropy ΔS. The negative value of ΔG is an example of the viability and spontaneity of the adsorption process. Positive value of ΔH indicated that the nature of process is endothermic, while the positive ΔS confirm the perfect affinity of adsorbate to adsorbent [33] .

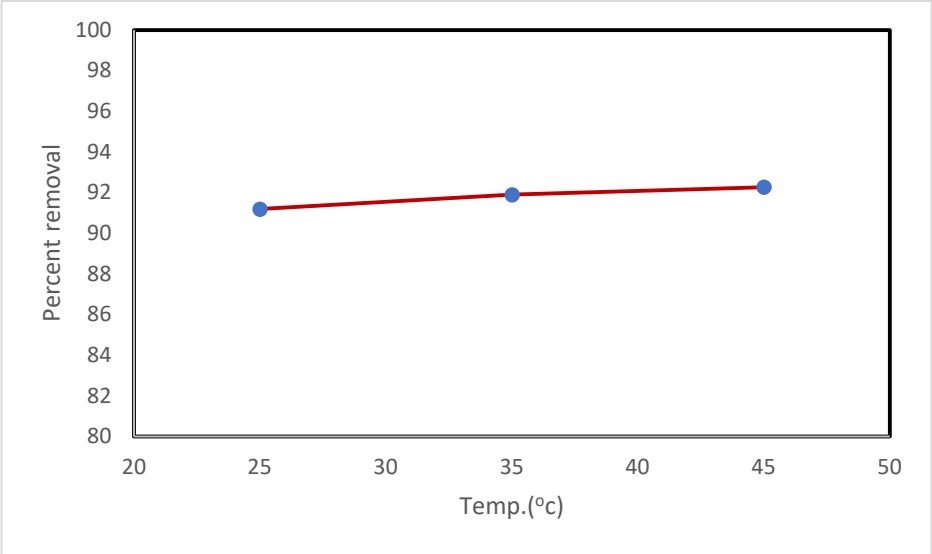

Figure 10 : Effect of temperature on CIP removal efficiency; Co(50)mg/l, particle size(424)µm, Temp.(25)ºC, dosage(0.02)g/ml, time of 80 min and rpm 300.

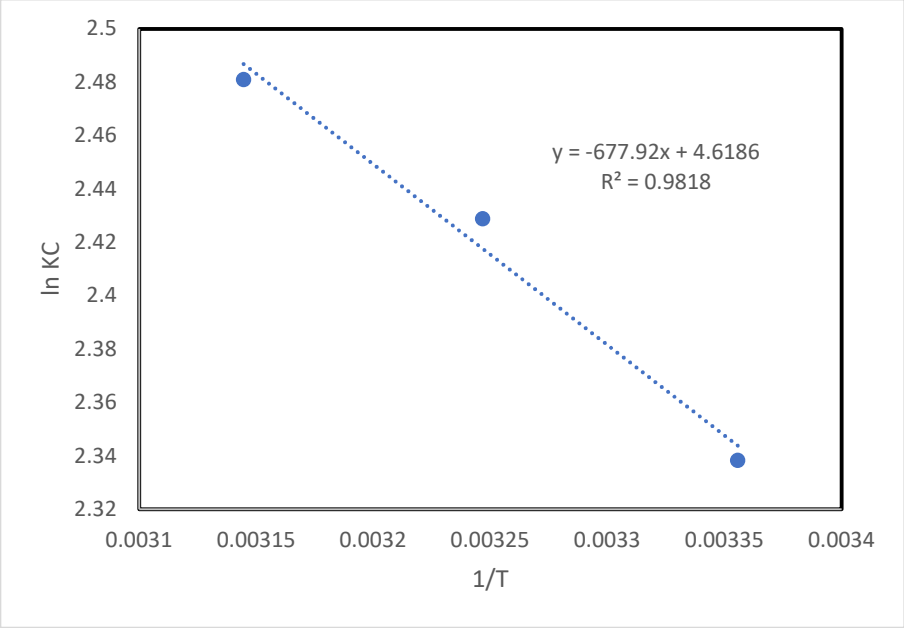

Figure 11 : Relationship between lnKd vs. 1/T for thermodynamic constants determination for CIP removal efficiency; Co=70 mg/l, particle size= 424 µm, T=25 °C, dosage= 0.02g/l, t= 120 min and rpm 300.

Table 5 : Thermodynamic parameters of CIP adsorption onto PC

1/T	Kc	Ln (Kc)	ΔG(kj/mol)	ΔH(kj/mol)	ΔS(kj/mol)	R2
0.003356	2.338303	0.849426	-2.10451290	5.63622688	0.03839904	0.9818
0.003247	2.428837	0.887413	-2.27240791			
0.003145	2.481013	0.908667	-2.40238099			

4.4 Isotherm Study

The well-known expression of the Langmuir model is given by Eq. (6) [19]:

$$q_e = \frac{q_m\, b_l C_e}{1+b_l C_e} \qquad (6)$$

Where, C_e, q_e, q_m, and b_l are the concentrations of reactive dyes at equilibrium (mg L^{-1}), the capacity of adsorption at equilibrium (mg g^{-1}), the maximum capacity of adsorption (mg g^{-1}) related to the Langmuir equilibrium constant, and shows quantitatively the convergence between CIP PC (L mg^{-1}), respectively. The Langmuir isotherm may be insufficient to fully explain the equilibrium form of heterogeneous adsorption mechanisms forming in single-layer adsorption. The basic characteristic of the Langmuir equation may be stated as the dimensionless differentiation factor (R_L) was used. R_L is a dimensionless constant, shown in Eq. (7) [12].

$$R_L = \frac{1}{1+K_L C_O} \qquad (7)$$

Here C_0 (mg/L) is initial dye concentration. If R_L is larger than 1, the adsorption process is unfavorable, if it is equal to 1 it is linear and if it has a value between 0 and 1 it is favorable (occurs spontaneously) and if it is 0 it is irreversible [16].

The Freundlich isotherm describes equilibrium on heterogeneous surfaces and hence does not assume monolayer capacity. Freundlich can be used for a broader range of pollutant concentrations and acceptable theoretical data requirements with experimental data calculated. It has been used in the current study. The isotherm is described by the following equations[8]:

$$q_e = K_f C_e^{1/n} \quad (8)$$

Where k_f and n are Freundlich constants and were calculated from the slope and intercept of the Freundlich plots. It has been shown that n values between 1 and 10 represent good adsorption potential of the adsorbent [14].

The models of adsorption isotherm are followed to define the distribution of the adsorbate among the adsorbent surface . A set of isotherm model assumptions are made in relation to the heterogeneity or homogeneity, coverages, and possibility of interaction. Langmuir isotherm and Freundlich Isotherm were examined for the equilibrium data to describe how the adsorbate molecules interaction with adsorbent surface. Also, to gives a comprehensive understanding of nature of interaction as showed in figure 12 . Table 6 shows the parameters values of the models with the correlation coefficient (R^2); q_{max} represent the maximum uptake of pollutant under a given condition, b a constant that represent the affinity between the sorbent and sorbate. K, and n are Freundlich constants which associated with the maximum adsorption capacity and intensity of adsorption respectively. The maximum adsorption capacity of CIP onto PC is 20.21 mg/g state that the prepared PC has a higher capacity of CIP adsorption. From the value of RL ($0<RL<1$) which is mean the adsorption is favorable process. Also independent on the value of n (i.e., Freundlich intensity) ($n>1$) know that the adsorption is preferential. Langmuir Model is the more fitted model that has the largest value of R^2 in the experiments works as show in table 6 . From the results of the maximum adsorption value, the porcelanite appeared good adsorbent for adsorption of CIP from aqueous solution in comparison with other adsorbents as shown in table 7.

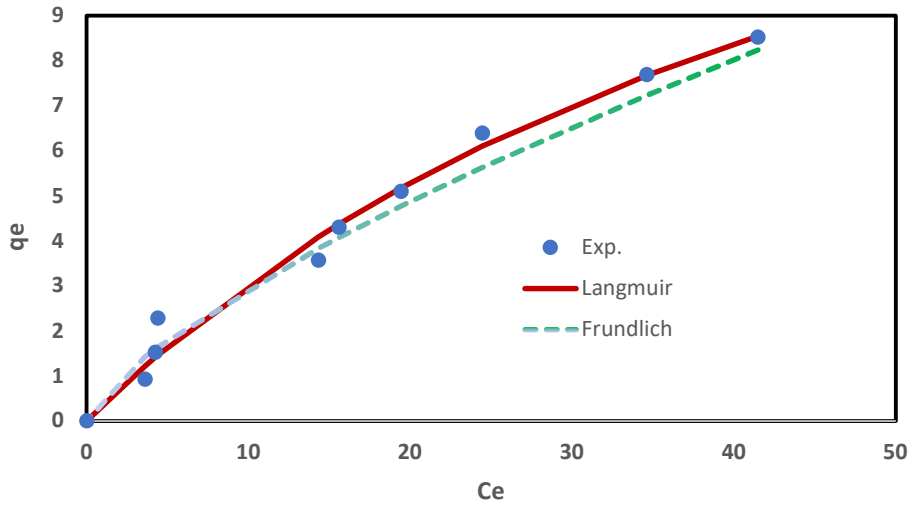

Figure 12 : Isotherm models for sorption of CIP onto PC

Table 6 : parameters values of the Isotherm models

Model	Parameters	Values
Freundlich Model	**K_f** **n** **R2** **1/n**	**0.564961** **1.39016** **0.9717** **0.71935**
Langmuir Model	**q_{max}** **Kl** **R2** **RL**	**20.20977** **0.017676** **0.985397** **0.530838**

Table 7. maximum adsorption capacity of CIP onto different adsorbents.

Adsorbate	Adsorbent	Max.Adsorption Capacity q_m (mg/g)	Ref.
CIP	Activated carbon derived from pomegranate peel wastes	2.353	Elhussien et al.,2017[124]

CIP	groundnut (Arachis hypogaea) shell powder and ZnO nanoparticles	8.07	Dhiman and Sharma,2018[125]
CIP	Fe3O4 nanoparticles	3.46	Khoshnamv et al.,2017[127]
CIP	Rice Husk	3.984	Ata et al(2022)
CIP	Humic acid/cellulose	10.86	. Wang L,(2020)
CIP	water hyacinth biochar	2.717	Ngeno,E,C(2016)
CIP	ZnO nanoparticles	0.160	Dhiman,N.(2019)
CIP	Porcilanite(PC)	20.21	This work

4.5 Kinetic Study

In order to examine the controlling mechanism and dynamics of the CIP and RR195 dyes adsorption process, the Lagergren pseudo-first-order, the pseudo-second-order and intraparticle diffusion [12] kinetic models were applied to experimental data.

The pseudo-first-order model is presented by the following equation[12]:

$$ln(q_e - q_t) = ln\, q_e - k_1 t \quad (9)$$

The plot of $ln(qe - qt)$ against t provides a linear relationship from which k_1, constant of pseudo-first-order adsorption (min^{-1}) (**Fig.13**) and q_e, adsorption capacity at equilibrium (mg g^{-1}) are determined from the slope and intercept of the plot, respectively, given that q_t is the adsorption capacity at time t (mg g^{-1}).

The pseudo-second-order kinetic rate equation is expressed as [6,12]

$$\frac{t}{q_t} = \frac{1}{k_2\, q_2^2} + \frac{1}{q_2} t \quad (10)$$

Where k_2 (g/mg min) is the rate constant of pseudo-second-order adsorption and q_2 is the equilibrium adsorption capacity (mg g^{-1}). Values of k_2 and q_2 were calculated from a plot of t/q_t against t (**Fig. 14**).

Adsorption has recently experienced extensive research as a practical way to remove a variety of hazardous substances from aqueous solutions, such as dyes and heavy metals [34, 35]. The majority

of adsorption research has focused mainly on kinetic processes. The kinetic data analysis is important for the adsorption process because its show way of adsorbate uptake rate, which controls the resident time in the adsorbent [35]. The percentage at which pollutants are take out from the aqueous solution is called adsorption kinetics. Also, the kinetics analysis is important to evaluate the effectiveness of adsorption and to explain by which process the adsorption phenomena is takes place, as well as, deliver dynamic evidence for the time required to reach equilibrium, the adsorption rate, and limiting step of the adsorption rate. If the adsorbent is targeted for use in facilities of wastewater treatment; a high adsorption rate is necessarily characteristic in addition to its adsorption ability and the removal efficiency [36].

The kinetics study of CIP adsorption was examined by pseudo first-order, pseudo second-order, and intra-particle diffusion model were using figures 13 and 14. The calculated parameter values were obtained by using these models in accordance with Eqs (6,7) are tabulated in Tables 8 . The most advantageous model is identified by comparing R^2 for each applied model and the accuracy between the calculated and experimental qe values . These kinetic model parameters were determined using nonlinear regression in Microsoft excel 2016. The higher values of R^2 and the values of theoretical qe which are near to the experimental qe, indicated that the second-order model is appropriate to adsorption behaver of CIP. Furthermore, the C values were greater than zero confirming that adsorption process rate limiting contribute to the diffusion of the boundary layer, not intra-particular diffusion [37, 38].

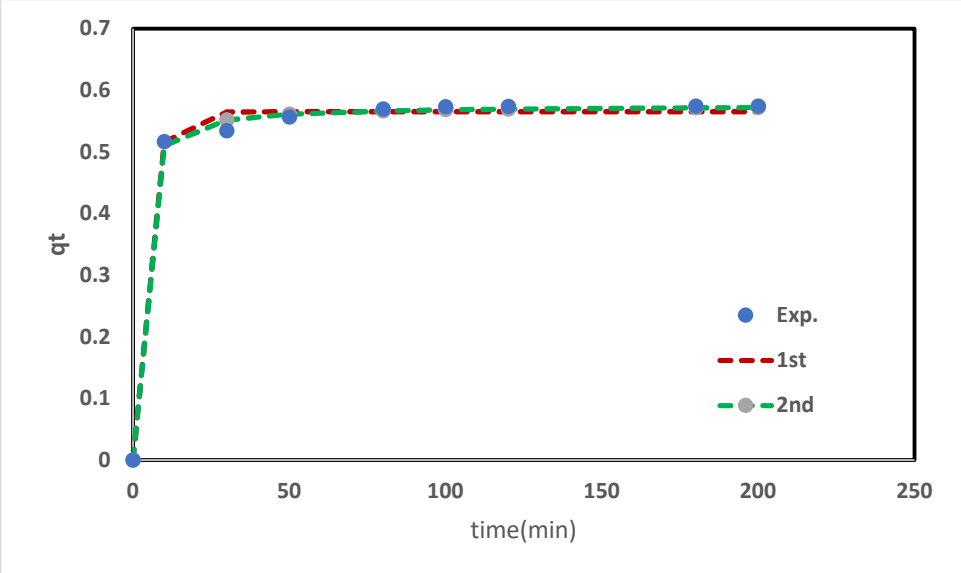

Figure 13: Pseudo-first-order for CIP onto PC

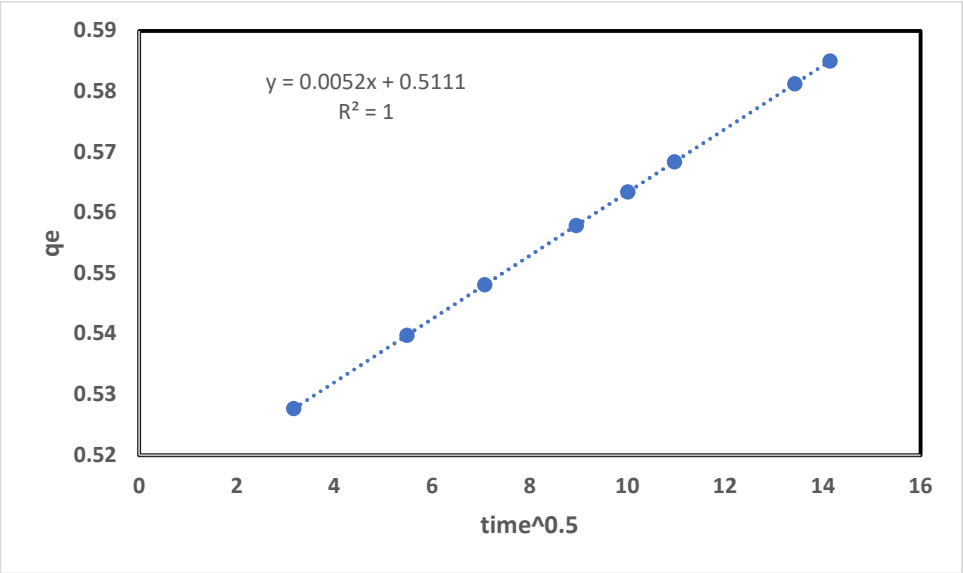

Figure 14 : Pseudo-second-order for CIP onto PC

Table 8 : parameters values of the Kinetic models

Model	Parameters	Values
Pseudo- first order	**K1** **R^2**	**0.244** **0.995**
Pseudo- second order	**K_2** **R^2**	**1.357** **0.9982**
Intraparticle diffusion	**C** **K_P** **R^2**	**0.511141** **0.005** **0.998**

5. Conclusion

The most considerable conclusions attained from the using of PC to treat synthesis wastewater with ciprofloxacin in batch and continues system mode can be listed below: FTIR analysis shows that the bands of silanol-OH and Si-OH-Si groups shifted to upper displacement and therefore it plays the major role in adsorption process. XRD pattern result that the mainly PC compound is quartz with a chemical formula SiO_2. Also, there is no obvious difference between XRD peaks of adsorbent before and after adsorption mean that there was no change in the chemical composition of the PC and the removal process is a physisorption. Surface morphology shows a wide variety of size and shape of intergranular pores relatively to the high porosity of PC also, indicating high surface areas. In contrast, the high ratio of Si before and after adsorption made the EDS analysis compatible with the FTIR (The major functional groups present in the samples were Si-O-Si groups) and XRD (The mainly compound is quartz with a chemical formula SiO_2. In batch

system mode; the optimal pH was around 5. The optimum dose is 0.02 g/ml because it gives a suitable removal by the consumption of a fit amount of PC. Results show that the removal efficiency decreased with the increased in particle size and the best removal efficiency (92.5 %) was at the particles size of 425 μm. The CIP adsorbing was rather fast in the first min and reach to the state of equilibrium was at 80 min. The removal efficiencies of CIP increased dramatically as the initial concentration increased and the best removal percent was 92.5% at 60 mg/l. The results were improved using the regression equation of response value gives best removal percent by surface method (RSM) with central composite design (CCD). All the results of RMS are really closed to that of batch experiments. From this result; the optimal condition through the experiments of continuous operation mode can be choice as(pH=5.322, dose= 0.02196 g/ml, particle size=425 μm, initial concentration of 58.7002mg/l, time= 80.88 min and temperature of 25ºC) at shaking speed of 300rpm which gives 92.5% of CIP adsorption. There is no significant effect of temperature on the CIP adsorption. Removal percent slightly increase with temperature increasing revealed that CIP adsorption is endothermic. The negative value of ΔG represent the viability and spontaneity of adsorption process. Positive value of ΔH indicated that the nature of process is endothermic, while the positive ΔS confirm the perfect affinity of adsorbate to adsorbent. Isotherm study state that the maximum adsorption capacity of CIP onto PC is 20.21 mg/g. RL value ($0<RL<1$) state the adsorption is favorable process. Freundlich intensity ($n>1$) suggested that the adsorption is preferential. Langmuir Model is the more fitted model that has the largest value of R^2 of (0.98539). Both the first-order kinetic model fitted with R2=0.995 and the Second-order kinetic model with R^2=0.998 are appropriate although the Second-order kinetic more fitted to describe the adsorption behavior of CIP. Furthermore, the C values of the Intraparticle diffusion model were greater than zero confirming that adsorption process rate limiting contributes to the diffusion of the boundary layer, not intra-particular diffusion.

References

[1] Rahmani, A. R., Nematollahi, D., Samarghandi, M. R., Samadi, M. T., & Azarian, G. (2018). A combined advanced oxidation process: Electrooxidation-ozonation for antibiotic ciprofloxacin removal from aqueous solution. Journal of Electroanalytical Chemistry, 808, 82-89.

[2] H. Jones, O. A., Voulvoulis, N., & Lester, J. N. (2005). Human pharmaceuticals in wastewater treatment processes. Critical reviews in environmental science and technology, 35(4), 401-427.

[3] Mohammed, S. J., & Mohammed-Ridha, M. J. (2021). Optimization of levofloxacin removal from aqueous solution using electrocoagulation process by response surface methodology. Iraqi Journal of Agricultural Sciences, 52(1), 204-217.

[4] Genç, N., Can Dogan, E., & Yurtsever, M. (2013). Bentonite for ciprofloxacin removal from aqueous solution. Water science and technology, 68(4), 848-855.

[5] Rakshit, S., Sarkar, D., Elzinga, E. J., Punamiya, P., & Datta, R. (2013). Mechanisms of ciprofloxacin removal by nano-sized magnetite. Journal of hazardous materials, 246, 221-226.

[6] Wang, C. J., Li, Z., Jiang, W. T., Jean, J. S., & Liu, C. C. (2010). Cation exchange interaction between antibiotic ciprofloxacin and montmorillonite. Journal of Hazardous Materials, 183(1-3), 309-314.

[7] Mohammed, S. J., M-Ridha, M. J., Abed, K. M., & Elgharbawy, A. A. (2021). Removal of levofloxacin and ciprofloxacin from aqueous solutions and an economic evaluation using the electrocoagulation process. International Journal of Environmental Analytical Chemistry, 1-19.
[8] Moussavi, G., Alahabadi, A., & Yaghmaeian, K. (2015). Investigating the potential of carbon activated with NH4Cl for catalyzing the degradation and mineralization of antibiotics in ozonation process. Chemical Engineering Research and Design, 97, 91-99.
[9] Tunc, S. E., Aksu, K., Keser, G., Oksel, F., Doganavsargil, E., Pirildar, T., ... & Huseyinov, A. (2005). Platelet-activating factor and P-selectin activities in thrombotic and nonthrombotic Behçet's patients. Rheumatology international, 25(5), 326-331.
[10] Wang, Y. J., Jia, D. A., Sun, R. J., Zhu, H. W., & Zhou, D. M. (2008). Adsorption and cosorption of tetracycline and copper (II) on montmorillonite as affected by solution pH. Environmental Science & Technology, 42(9), 3254-3259.
[11] DeWitte, B., Dewulf, J., Demeestere, K., Van De Vyvere, V., De Wispelaere, P., & Van Langenhove, H. (2008). Ozonation of ciprofloxacin in water: HRMS identification of reaction products and pathways. Environmental science & technology, 42(13), 4889-4895.
[12] Ibrahim, M. A., Shaban, M. A. A., Hasan, Y. R., Hussein, H. A., Abed, K. M., Mohammed, S. J., ... & Hasan, H. A. (2022). Simultaneous Adsorption of Ternary Antibiotics (Levofloxacin, Meropenem, and Tetracycline) by SunFlower Husk Coated with Copper Oxide Nanoparticles. Journal of Ecological Engineering, 23(6).
[13] Liu, Y., Gan, X., Zhou, B., Xiong, B., Li, J., Dong, C., ... & Cai, W. (2009). Photoelectrocatalytic degradation of tetracycline by highly effective TiO2 nanopore arrays electrode. Journal of Hazardous Materials, 171(1-3), 678-683.
[14] Massé, D. I., Cata Saady, N. M., & Gilbert, Y. (2014). Potential of biological processes to eliminate antibiotics in livestock manure: an overview. Animals, 4(2), 146-163.
[15] Yoosefian, M., Ahmadzadeh, S., Aghasi, M., & Dolatabadi, M. (2017). Optimization of electrocoagulation process for efficient removal of ciprofloxacin antibiotic using iron electrode; kinetic and isotherm studies of adsorption. Journal of Molecular Liquids, 225, 544-553.
[16] Salman, M. S., Alhares, H. S., Ali, Q. A., M-Ridha, M. J., Mohammed, S. J., & Abed, K. M. (2022). Cladophora algae modified with CuO nanoparticles for tetracycline removal from aqueous solutions. Water, Air, & Soil Pollution, 233(8), 321.
[17] C. Namasivayam, R. Radhika, and S. Suba, "Uptake of dyes by a promising locally available agricultural solid waste: coir pith," Waste Manag., vol. 21, no. 4, pp. 381–387, 2001.
[18] M. Özacar and İ. A. Şengil, "Adsorption of reactive dyes on calcined alunite from aqueous solutions," J. Hazard. Mater., vol. 98, no. 1–3, pp. 211–224, 2003.
[19] Alhares, H. S., Shaban, M. A. A., Salman, M. S., M-Ridha, M. J., Mohammed, S. J., Abed, K. M., ... & Hasan, H. A. (2023). Sunflower Husks Coated with Copper Oxide Nanoparticles for Reactive Blue 49 and Reactive Red 195 Removals: Adsorption Mechanisms, Thermodynamic, Kinetic, and Isotherm Studies. Water, Air, & Soil Pollution, 234(1), 35.

[20] Ma, Q. Y., Logan, T. J., & Traina, S. J. (1995). Lead immobilization from aqueous solutions and contaminated soils using phosphate rocks. *Environmental Science & Technology*, *29*(4), 1118–1126.

[21] Boussaa, S., Kheloufi, A., Zaourar, N. B., & Kerkar, F. (2016). Valorization of Algerian Sand for Photovoltaic Application. *Acta Physica Polonica, A.*, *130*(1).

[22] Faisal, A. A. H., Al-Wakel, S. F. A., Assi, H. A., Naji, L. A., & Naushad, M. (2020). Waterworks sludge-filter sand permeable reactive barrier for removal of toxic lead ions from contaminated groundwater. *Journal of Water Process Engineering*, *33*, 101112.

[23] Afaj, A. H., & Mohammad, M. R. (2015). Removal of phenol from industrial effluents using activated carbon and Iraqi Porcelanite rocks–A comparative study. *Journal of the College of Basic Education*, *21*(91), 21–32.

[24] AL-Rubaeey, E. T. K., & AL-Myali, R. A. J. (2013). Thermodynamic study of adsorption of azure dyes on Iraqi porcelanite rocks. *J. Nat. Sci. Res.*, *3*, 68–72.

[25] Yao, Z.-Y., Qi, J.-H., & Wang, L.-H. (2010). Equilibrium, kinetic and thermodynamic studies on the biosorption of Cu (II) onto chestnut shell. *Journal of Hazardous Materials*, *174*(1–3), 137–143.

[26] Özsin, G., Kılıç, M., Apaydın-Varol, E., & Pütün, A. E. (2019). Chemically activated carbon production from agricultural waste of chickpea and its application for heavy metal adsorption: equilibrium, kinetic, and thermodynamic studies. *Applied Water Science*, *9*(3), 1–14.

[27] Sun, Y., Yue, Q., Gao, B., Wang, B., Li, Q., Huang, L., & Xu, X. (2012). Comparison of activated carbons from Arundo donax Linn with H4P2O7 activation by conventional and microwave heating methods. *Chemical Engineering Journal*, *192*, 308–314.

[28] Kareem, S. L., & Mohammed, A. A. (2020). Removal of Tetracycline from Wastewater Using Circulating Fluidized Bed. *Iraqi Journal of Chemical and Petroleum Engineering*, *21*(3), 29–37.

[29] Mohammed, A. A., & Kareem, S. L. (2019). Adsorption of tetracycline fom wastewater by using Pistachio shell coated with ZnO nanoparticles: Equilibrium, kinetic and isotherm studies. *Alexandria Engineering Journal*, *58*(3), 917–928.

[30] Gupta, A., Mahajan, S., & Sharma, R. (2015). Evaluation of antimicrobial activity of Curcuma longa rhizome extract against Staphylococcus aureus. *Biotechnology Reports*, *6*, 51–55.

[31] M-Ridha, M. J., Zeki, S. L., Mohammed, S. J., Abed, K. M., & Hasan, H. A. (2021). Heavy metals removal from simulated wastewater using horizontal subsurface constructed wetland. Journal of Ecological Engineering, 22(8), 243-250.

[32] Doğan, M., & Alkan, M. (2003). Adsorption kinetics of methyl violet onto perlite. *Chemosphere*, *50*(4), 517–528.

[33] Banerjee, S., & Chattopadhyaya, M. C. (2017). Adsorption characteristics for the removal of a toxic dye, tartrazine from aqueous solutions by a low cost agricultural by-product. *Arabian Journal of Chemistry*, *10*, S1629–S1638.

[34] Elhussien, M. E., lraheem, M. A.A., Hussein, R.M., & Elsaim, M.H., (2017). Removal of Ciprofloxacin Hydrochloride from Aqueous Solution by Pomegranate Peel Grown in Alziedab Agricultural Scheme - River Nile State, Sudan. Advances in Biochemistry, 5(5), 89-96.
[35] M-Ridha, M. J., Faeq Ali, M., Hussein Taly, A., Abed, K. M., Mohammed, S. J., Muhamad, M. H., & Abu Hasan, H. (2022). Subsurface Flow Phytoremediation Using Barley Plants for Water Recovery from Kerosene-Contaminated Water: Effect of Kerosene Concentration and Removal Kinetics. Water, 14(5), 687.
[36] Dhiman, N., & Sharma, N. (2018). Batch adsorption studies on the removal of ciprofloxacin hydrochloride from aqueous solution using ZnO nanoparticles and groundnut (Arachis hypogaea) shell powder: a comparison. Indian Chemical Engineer, 1–10.
[37] Aziz, G. M., Hussein, S. I., M-Ridha, M. J., Mohammed, S. J., Abed, K. M., Muhamad, M. H., & Hasan, H. A. (2023). Activity of laccase enzyme extracted from Malva parviflora and its potential for degradation of reactive dyes in aqueous solution. Biocatalysis and Agricultural Biotechnology, 102671.
[38] N. Dhiman, N. Sharma, Removal of pharmaceutical drugs from binary mixtures by use of ZnO nanoparticles: (competitive adsorption of drugs), Environ. Technol. Innovation, 15 (2019) 100392, doi: 10.1016/j.eti.2019.100392.